

DEEP-SEA SCLERACTINIAN CORAL AGE AND DEPTH DISTRIBUTIONS IN THE NORTHWEST ATLANTIC FOR THE LAST 225,000 YEARS

*Laura F. Robinson, Jess F. Adkins, Daniel S. Scheirer,
Diego P. Fernandez, Alexander Gagnon, and Rhian G. Waller*

ABSTRACT

Deep-sea corals have grown for over 200,000 yrs on the New England Seamounts in the northwest Atlantic, and this paper describes their distribution both with respect to depth and time. Many thousands of fossil scleractinian corals were collected on a series of cruises from 2003–2005; by contrast, live ones were scarce. On these seamounts, the depth distribution of fossil *Desmophyllum dianthus* (Esper, 1794) is markedly different to that of the colonial scleractinian corals, extending 750 m deeper in the water column to a distinct cut-off at 2500 m. This cut-off is likely to be controlled by the maximum depth of a notch-shaped feature in the seamount morphology. The ages of *D. dianthus* corals as determined by U-series measurements range from modern to older than 200,000 yrs. The age distribution is not constant over time, and most corals have ages from the last glacial period. Within the glacial period, increases in coral population density at Muir and Manning Seamounts coincided with times at which large-scale ocean circulation changes have been documented in the deep North Atlantic. Ocean circulation changes have an effect on coral distributions, but the cause of the link is not known.

The deep ocean has an important role in modulating global climate: its circulation transports heat across the equator and it acts as the major sink for carbon dioxide. During the last million years two dramatic types of climate change are obvious in geologic records, 100,000 yr glacial-interglacial oscillations (Imbrie et al., 1984) and abrupt millennial scale climate changes during the last glacial period (Grootes et al., 1993). The mechanisms driving these climate oscillations have not yet been fully explained, but it is likely that ocean circulation is critical to both (Broecker, 1998).

Geochemical reconstructions have demonstrated that circulation in the glacial Atlantic was different than today (Duplessy et al., 1988; Oppo and Lehman, 1993; Curry and Oppo, 2005). At the latitude of the New England Seamounts, northern-source deep water shoaled to ~2000 m water depth and was replaced by southern-source water. During the deglaciation the climate switched between warm and cool conditions (Grootes et al., 1993). At the same time the North Atlantic circulation pattern switched between glacial-like and modern-like circulation pattern (Boyle and Keigwin, 1987; Marchitto et al., 1998). At intermediate depths (< 2500 m) ocean circulation was also variable, with large changes in water-mass properties occurring on decadal timescales, but these changes were not always associated with the most obvious climate events (Robinson et al., 2005).

One of the most striking records of climate changes in North Atlantic marine sediments is the presence of Heinrich events, characterized by anomalous occurrences of ice-rafted debris (Heinrich, 1988). The large volumes of fresh water associated with melting ice may have decreased the rate of North Atlantic Deep Water (NADW) formation, together with a slow down in the overall ventilation rate of the oceans (Rahmstorf, 1995). Strong evidence in the form of ($^{231}\text{Pa}/^{230}\text{Th}$) ratios recorded in

deep-sea sediments support just such a reduction in the circulation rate of NADW at Heinrich event 1 and the Younger Dryas (McManus et al., 2004).

Since about half of the deep-water formation in the modern ocean occurs in the North Atlantic (Broecker et al., 1998; Ganachaud and Wunsch, 2000), the northwest Atlantic basin is a location of particular interest for investigating the links between ocean circulation and climate. However, constructing high-resolution deep-sea records can be challenging because sedimentary cores tend to be mixed by bioturbation, smoothing the signals of rapid change in the deep ocean. One way to alleviate this difficulty is to analyze the chemical composition of deep-sea coral skeletons.

Deep-sea corals have been found at depths ranging from 0 to 5000 m in all of the major ocean basins (Freiwald, 2002). The chemical composition of the aragonite skeletons of scleractinian corals is affected by: (a) the composition of the seawater in which they grow, (b) environmental parameters, such as temperature, and (c) biological vital effects (Shen and Boyle, 1988; Smith et al., 1997; Adkins et al., 1998, 2003; Mangini et al., 1998; Cohen et al., 2001; Goldstein et al., 2001; Meibom et al., 2003; Schroder-Ritzrau et al., 2003; Frank et al., 2004; Bond et al., 2005; Robinson et al., 2005). Since corals live for long time periods, and their skeletons are preserved when they die, they form a unique archive of ocean conditions in the past. Indeed, multiple sub-samples taken carefully from one specimen can be used to generate a time series of changes that occurred in the ocean during the lifetime of the coral (Adkins et al., 1998). The high uranium content of aragonite (~3 ppm) makes some species of deep-sea coral well suited to precise U-Th analyses allowing absolute ages to be measured over many hundreds of thousands of years. Such dating allows us to link records from multiple fossil individuals to look at even longer time periods (Robinson et al., 2005).

The New England Seamounts are well located to capture variability in deep Atlantic circulation (Fig. 1). Both fossil and modern deep-sea corals were collected from these seamounts more than 45 yrs ago on RV ATLANTIS cruises 260 and 280. More recently over 3500 solitary and 10s of kilograms of colonial scleractinian corals (Fig. 2) were collected from the New England Seamounts in May/June 2003 (Adkins and Scheirer, 2003). Use of the deep submergence vehicle DSV ALVIN ensured that the depth of each coral was well known, and the corals were collected at, or near to, life position. Additional samples were collected during a second DSV ALVIN cruise and an remotely operated vehicle ROV HERCULES cruise in 2005, covering both the New England Seamounts and the Corner Rise Seamounts. Here we describe the distribution of deep-sea corals both with depth and time in the North Atlantic, and how they may be linked to changes in deep-water circulation. Understanding these changes is important when using corals for paleo-climate reconstructions, and also for understanding the modern day distribution of deep-sea coral populations.

METHODS

All samples were collected using deep submergence vehicles (DSV ALVIN or the ROV HERCULES) and a netted basket was used to "scoop" up corals from on the sea floor. Corals were counted, weighed, and archived at Caltech. A random selection of coral individuals from each depth and seamount was taken for U-series analysis. A potential bias in the final age distribution is that each coral selected must contain sufficient carbonate (i.e., biased towards larger individuals). A 0.5–1.0 g piece of carbonate was taken from each of 127 corals, with a total of 159 U-Th analyses. Visible ferromanganese crust was physically removed from each sample,

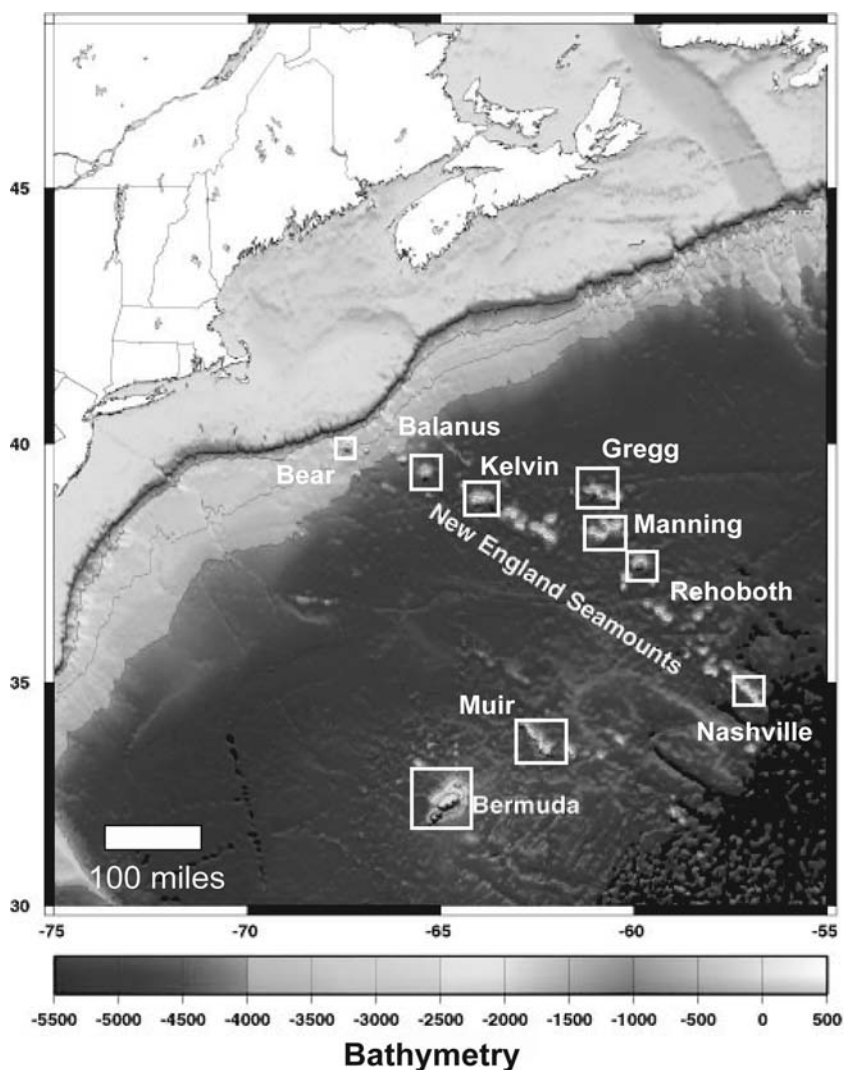


Figure 1. Map of New England Seamounts showing location of seamounts from which deep-sea corals were collected during three cruises from 2003–2006.

and holes formed by endolithic organisms were drilled out using a dremel tool. Each sample was subjected to a rigorous chemical cleaning procedure designed to remove the remaining ferromanganese crust (Cheng et al., 2000). Dissolved samples were spiked with a mixed ^{229}Th – ^{236}U spike, and U and Th were separated and purified by anion-exchange chemistry (Edwards et al., 1986). The spike ratio was calibrated to a 2 SD uncertainty of 0.4% using HU-1, a U-series standard close to secular equilibrium (Cheng et al., 2000). Purified aliquots of U and Th were measured by Neptune multi-collector inductively coupled mass spectrometer (MC-ICP-MS) with bracketing standards of CRM-145 for U, and an in-house Th standard calibrated against CRM-145 (Robinson et al., 2002, 2005). Procedural blanks had an average value of 67 pg for ^{238}U (< 0.002% of the typical sample size) and 2 fg for ^{230}Th . The ^{232}Th concentration in each sample was measured to quantify remaining contamination from Th-rich ferromanganese crust. This ^{232}Th -based estimate was used to correct for initial ^{230}Th using a $^{232}\text{Th}/^{230}\text{Th}$ ratio of $12,500 \pm 12,500$ (Cheng et al., 2000).

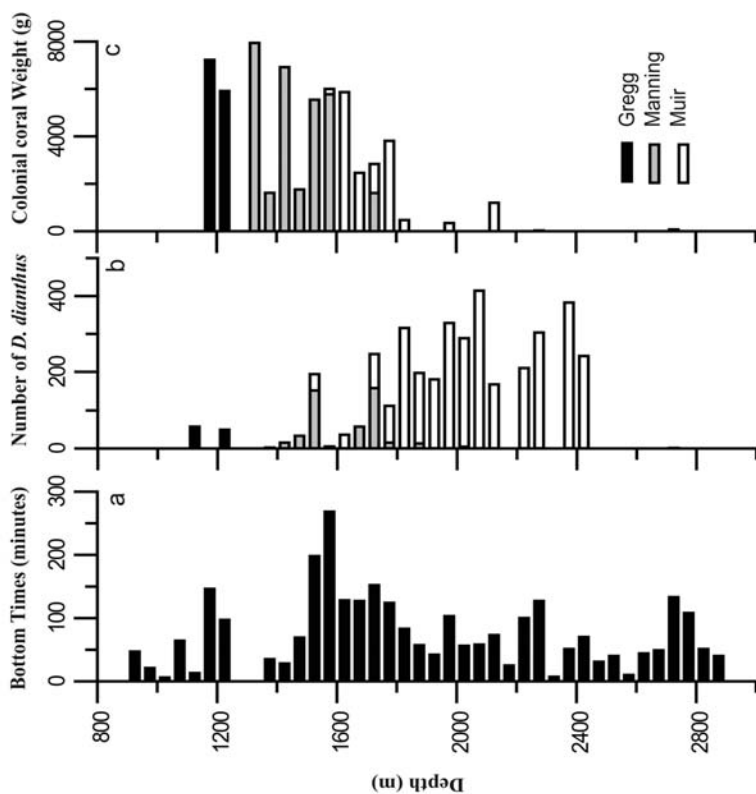


Figure 2. Depth distribution of the samples collected during the DSV ALVIN cruise to the New England Seamounts in 2003. (A) Time in minutes spent at the bottom; (B) number of *Desmophyllum dianthus* collected; and (C) weight of colonial corals collected, including *Enallopsammia*, *Lophelia*, and *Solenosmilia*. Although significant time was spent at depths > 2500 m, very few corals were recovered. Black bars are from Gregg Seamount, grey bars are from Manning Seamount, and white bars are from Muir Seamount.

RESULTS

Most of the samples discussed herein were collected in May/June 2003 on DSV ALVIN cruise AT7_35 to Manning, Muir, and Gregg Seamounts (Adkins and Scheirer, 2003) (Fig. 1). During 3190 min (53 hrs, 10 min) of DSV ALVIN bottom time ranging in depth from 920 to 2870 m, we collected more than 3700 individual fossil *Desmophyllum dianthus* (Esper, 1794) and more than 60 kg of colonial corals (Fig. 2). The deepest colonial fossil coral sample was collected from ~2750 m, but > 95% of samples ranged from 1175–1800 m. By contrast 99% of *D. dianthus* individuals were collected between 1175 m and 2550 m, with one deep sample collected at 2740 m (Fig. 2). At this location, the depth range of *D. dianthus*, reaches ~ 750 m deeper than the colonial scleractinians. In June 2003 further DSV ALVIN sampling (Cruise AT8-1.) on an Ocean Exploration cruise “Mountains in the Sea” recovered further fossil corals, including samples from Kelvin and Bear Seamounts (Fig. 1). The ROV HERCULES cruise in August 2005 recovered more than 1300 fossil *D. dianthus* corals from the New England Seamounts and the Corner Rise Seamounts. The fossil depth

distribution from Muir, Manning, Nashville, Rehoboth, Kelvin, Balanus, and Gregg Seamounts are similar, considering the depth ranges to which dives were made. Only 15 modern *D. dianthus* individuals were collected from all of the New England Seamounts (Fig. 3). The range of modern *D. dianthus*; 1600–2200 m is similar to the fossil distribution, but the small number of modern samples collected precludes a statistical depth comparison between the two sample sets.

All U-series analyses data are recorded in Table 1, and some of these data have been presented previously (Robinson et al., 2005, 2006). A measure of the extent of diagenetic alteration to the U-series system is the ($^{234}\text{U}/^{238}\text{U}$) ratio (where parentheses indicate activity ratio). Marine carbonates incorporate the isotopic ratio (denoted as $\delta^{234}\text{U} = ([(^{234}\text{U}/^{238}\text{U})_{\text{meas}} / (^{234}\text{U}/^{238}\text{U})_{\text{eq}}] - 1) \times 10^3$) of the seawater in which they grow (Broecker and Takahashi, 1966; Robinson et al., 2004). This value is invariant throughout the water column (Cheng et al., 2000) and has been constant ($\sim 146\%$) to within $\sim 10\%$ over the last several hundred thousand years (Bard et al., 1991; Stirling et al., 1995; Henderson, 2002; Robinson et al., 2004). For a closed-system, the $\delta^{234}\text{U}_{\text{initial}}$ ($\delta^{234}\text{U}_{\text{initial}} = \delta^{234}\text{Ue}^{\lambda t}$) should be identical to that of the modern day (Edwards et al., 1986). Samples with $\delta^{234}\text{U}_{\text{initial}}$ values different to modern seawater are likely to return inaccurate apparent ages (Gallup et al., 1994). Such changes may come about through processes such as open-system exchange with seawater or U-rich organic matter, or through internal re-arrangement of alpha-recoil mobilized ^{234}U (e.g., Robinson et al., 2006). All of the data in the discussion focuses on samples with $\delta^{234}\text{U}_{\text{initial}}$ values within 7‰ of modern seawater. Twenty-eight out of 127 corals lie outside the acceptable range (Table 2). Reliable ages range from 225–0.3 ka for *D. dianthus* (Fig. 4; $n = 93$), 12.6–11.7 ka for *Caryophyllia* ($n = 2$), 0.1–0.08 ka for *Solenosmilia* ($n = 2$), and 0.2 ka for *Enallopsammia* ($n = 1$). Ninety-six of these ages are from the Cruise AT7-35 (Adkins and Scheirer, 2003) and represent 2.7% of the sample collection from that cruise.

At one location we recovered a fallen gorgonian coral acting as a growth substrate for *D. dianthus*. Reliable ages for *D. dianthus* corals growing on the gorgonian range from 65 ka to 30 ka. Ages from the gorgonian itself were difficult to establish as the wide range of $\delta^{234}\text{U}_{\text{initial}}$ values (151.4‰–187.8‰) indicate that its skeleton is more prone to diagenesis than scleractinians (Table 1). We have not yet carried out extensive studies to determine the potential for U-series dating in gorgonian corals.

DISCUSSION

DEPTH DISTRIBUTION.—Attempts have been made to document the depth distributions of modern deep-sea corals (Freiwald, 2002), but the expense and logistical problems associated with exploring the deep-ocean floor has made a full inventory impossible. We know even less about the distributions of fossil deep-sea corals through depth or time. Our New England Seamount collection shows a distinct depth cut-off at 1800 m for colonial corals and 2500 m for *D. dianthus* in the fossil record. On Muir Seamount, most of the exploration was carried out in a deep notch between two peaks in the ridge. This notch provides a hard substrate and the seafloor experiences strong currents thought to be beneficial for coral growth. The maximum depth of the notch (2500 m) may be the cause of the paucity of scleractinian corals collected below 2500 m. A second notch farther east extends to much greater depths, and collections from this location would clarify whether the ridge morphology is

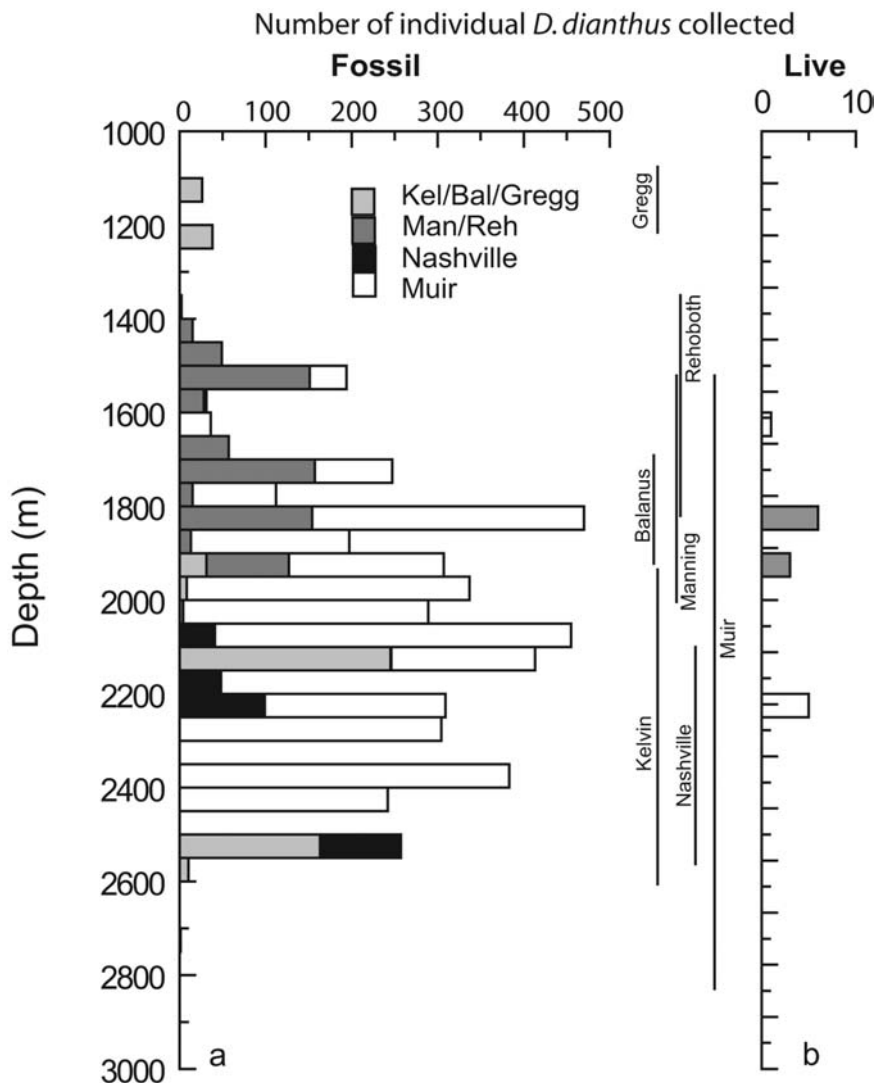


Figure 3. Depth distribution for fossil and live *Desmophyllum dianthus* collected during the DSV ALVIN cruise in 2003 and the ROV HERCULES cruise in 2005, highlighting the large number and depth range of fossil corals on all seamounts compared to live corals. The collection is only a subsample of the number of corals observed during these dives, especially with respect to fossil corals for which representative “scoops” of corals were taken from each sample site. The seamounts are grouped geographically, with Kelvin, Balanus, and Gregg the most northwesterly, Manning and Rehoboth in the middle of the chain, Nashville farther east, and Muir separate from the chain (see Fig. 1). Additional corals were collected from the Corner Rise Seamounts. The vertical lines demark the depths at which dives looking for corals took place. Few live specimens were recovered, despite focused searches to allow for modern studies.

indeed the major control on the depth distribution of *D. dianthus* collected on cruise AT7-35. This explanation, however, does not account for the depth distribution of the fossil colonial corals (*Solenosmilia*, *Lophelia*, and *Enallopsammia*) because they become less abundant at ~1800 m.

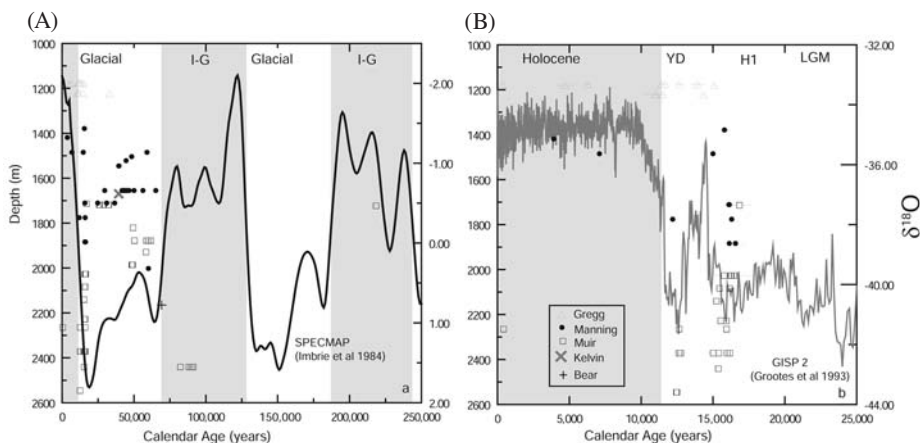


Figure 4. Ages and depths of dated fossil corals that have U-isotope ratios indicative of closed system behavior. (A) all of the dated *Desmophyllum dianthus* from Gregg, Manning, Bear, Kelvin, and Muir Seamounts. Ages range from 225 ka to modern. Additional age measurements from *Solenosmilia*, *Enallopsammia*, and *Caryophyllia* and from a gorgonian octocoral are shown in Table 1. The thick black line is the $\delta^{18}\text{O}$ SPECMAP curve (Imbrie et al., 1984) where more negative values are indicative of interglacial conditions (shaded grey) and more positive values are indicative of glacial times. The majority of the coral ages lie within the last glacial period. (B) an enlargement of the last glacial maximum, the deglaciation, and the Holocene (shaded grey). The grey curve is the $\delta^{18}\text{O}$ record from GISP 2 (Grootes et al., 1993). No corals have been found with ages within the Last Glacial Maximum (23–19 ka) as defined by the EPILOG working group (Mix et al., 2001).

A second factor that may impact the distribution of deep-sea corals is the properties of the water itself. The current velocity may affect either the range and distribution of coral larvae or the supply of food. Additionally, the properties of the water-mass bathing the seamount (e.g., nutrients, salinity or temperature) may be more or less beneficial to coral growth. The modern water column at the location of the New England Seamounts is filled by North Atlantic Deep Water (NADW), with no distinct depth gradients in nutrients, temperature, or salinity at the relevant depths. There is, therefore, no obvious water-mass property controlling the depth distribution of azooxanthellate scleractinians in the NW Atlantic today. However, at certain times in the past we know that the circulation pattern was different than the modern. For example, southern-sourced water was present up to depths of about 2000 m during the last glacial maximum (LGM) (Oppo and Lehman, 1993; Curry and Oppo, 2005). This water-mass boundary is close to the cut-off depth of *D. dianthus* and colonial scleractinians, suggestive of a link between ocean circulation and coral distribution. The best way to explore this relationship in detail is to examine the age distribution of the corals.

AGE DISTRIBUTION.—By looking at the ages of the New England Seamount *D. dianthus* populations we can learn more about the controls on their distribution, for example, whether the coral populations grew continuously over time, whether the population density was pulsed, and whether any such pulses are linked to known changes in the deep ocean. In the simplest case, the population has been stable. In the study area we found 15 live, and ~5000 fossil individuals. If we assume that each coral has a life span of ~100 yrs (Adkins et al., 2004) then a stable population could have persisted for ~35,000 yrs. We observe corals that are many times older than 35

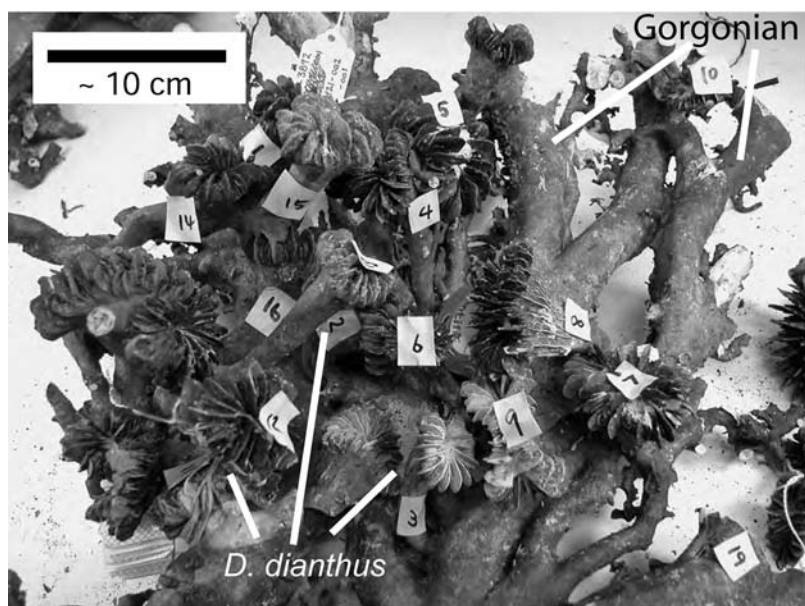


Figure 5. Portion of a deep-sea coral build up. At the base, a large fallen gorgonian skeleton was oriented horizontally. Multiple *Desmophyllum dianthus* corals have grown both on the fallen gorgonian, and upon one another. Much of the structure is coated in a black or brown ferromanganese crust. This buildup acts as a natural, long-lived recruitment experiment allowing us to investigate the relative timing of deep-sea coral settling.

ka, our first indication that the population has not in fact been stable. The age distributions of corals from Muir and Manning Seamounts appear to be different to those from Gregg Seamount and are discussed separately below (Fig. 4a).

MUIR AND MANNING SEAMOUNTS.—Visually, it is clear that the growth of these corals is not randomly distributed through time, but that most of the corals grew during the last glacial period—i.e., from 70 to 10 ka (Fig. 4A). On Muir Seamount, farthest to the south, there are only five corals that grew during interglacials, and four of these were alive during Marine Isotope Stage (MIS) 5b. MIS 5b is a stadial near to the end of the last interglacial period when the deep-ocean temperature had already changed to glacial-like conditions (Cutler et al., 2003). At Manning, only two corals have interglacial ages, both of which are from the Holocene (Fig. 4). At the first order, therefore, it appears that glacial conditions are most conducive to coral growth at these two sites.

An enlargement of the age distribution from the last glacial maximum (LGM) through to the Holocene shows pulses of population density. There are no corals from the Last Glacial Maximum [(23–19 ka as defined by the EPILOG working group (Mix et al., 2001)] and there are distinct increases in the number of corals at about 16.5 ka and 12.5 ka (Fig. 4B). In addition, there are increases in population density at around 44 ka and 40 ka (Fig. 6). The first of these pulses (44 ka) is well characterized by ages from the “slab” depicted in Figure 5. The *D. dianthus* corals growing on the gorgonian have a wide range of ages (65–30 ka) but 13 out of the 19 dated corals have ages between 44–42.5 ka.

The last glacial period and the subsequent deglaciation was characterized by unstable climate conditions compared to the Holocene (Grootes et al., 1993; Hughen et

Table 1. Uranium series data summary of concentrations and isotopic ratios. Calculated ages are reported before and after the ²³⁰Th_{initial} correction, and are in years before date of analysis (2004). Those samples in bold and marked by an asterisk are within 7% of the modern-day δ²³⁴U_{initial} seawater value (146‰). Database ID is a unique identifier for each deep-sea coral consisting of the Alvin dive, time of collection, station number and individual coral sample. All errors are 2 SE and are reported in unlabeled columns after each value. All corals are *D. dianthus* unless marked; C = *Caryophyllia*, E = *Enalltopsanninia*, S = *Solenosmilia*, and Go = Gorgonian. Analyses made on the gorgonian coral that forms “The slab” are italicized. Shading highlights replicate measurements from the same coral individual.

Lab ID	Database ID	Smt.	Depth (m)	238U (ppm)	230Th (ppt)	232Th (ppb)	δ ²³⁴ U _{present} ‰	(²³⁰ Th/ ²³⁸ U) activity	Raw age (yrs)	Corr age (yrs)	U _{initial} ‰							
UAG01	ALV-3905-BEAR-112-SS02 (bag 1)	Bear	2,165	3,522	0.001 31.39	0.13	8,220	0.438	124.4	1.2	0.5446	0.0023	71,255	442	69,182	2,059	151.2	1.7
UAG03	ALV-3905-BEAR-112-SS03 (bag 1)	Bear	2,165	3,444	0.001 31.37	0.13	25,869	0.435	128.7	1.2	0.5565	0.0024	73,020	458	66,443	6,130	155.3	3.1
UAF19	ALV-3905-BEAR-112(S)	Bear	2,165	2,830	0.002 27.73	0.12	40,529	0.177	129.4	1.1	0.5988	0.0026	80,991	531	67,945	11,434	156.8	5.3
UAJ05	ALV-3891-1459-003-002*	Gregg	1,176	4,496	0.002 8.39	0.04	0.878	0.006	139.6	1.1	0.1140	0.0005	11,486	55	11,378	118	144.2	1.1
UAJ11	ALV-3891-1459-003-004*	Gregg	1,176	3,766	0.003 8.71	0.04	3.214	0.015	142.6	1.2	0.1413	0.0007	14,379	74	13,906	461	148.3	1.2
UAM07	ALV-3891-1459-003-006-001* C	Gregg	1,176	4,116	0.002 8.65	0.04	2,499	0.016	143.8	1.2	0.1284	0.0006	12,971	63	12,638	328	149.1	1.2
UAM08	ALV-3891-1459-003-006-002* C	Gregg	1,176	4,682	0.002 9.25	0.04	3.551	0.019	144.8	1.1	0.1207	0.0005	12,135	58	11,724	400	149.7	1.2
UAM05	ALV-3891-1459-003-007*	Gregg	1,176	4,188	0.005 8.08	0.04	1.617	0.022	144.9	1.4	0.1178	0.0005	11,833	58	11,623	212	149.7	1.4
UAM04	ALV-3891-1459-003-009	Gregg	1,176	3,636	0.003 9.69	0.04	1.925	0.015	150.1	1.2	0.1629	0.0007	16,626	81	16,327	302	157.1	1.3
UAO19	ALV-3891-1459-003-009	Gregg	1,176	3,605	0.002 9.36	0.04	0.655	0.019	157.0	1.1	0.1587	0.0007	16,059	77	15,960	123	164.3	1.1
UAM06	ALV-3891-1459-003-011*	Gregg	1,176	3,617	0.002 0.22	0.00	0.292	0.011	148.2	1.1	0.0037	0.0000	354	2	315	35	148.3	1.1
UAL05	ALV-3891-1459-003-013*	Gregg	1,176	3,734	0.002 3.99	0.02	1.290	0.010	141.7	1.1	0.0654	0.0003	6,430	30	6,251	176	144.3	1.2
UAF18	ALV-3891-1459-003-B5* S	Gregg	1,176	3,330	0.002 0.07	0.00	0.390	0.012	149.2	1.2	0.0014	0.0000	130	3	75	32	149.3	1.2
UAK16	ALV-3891-1546-004-003*	Gregg	1,180	3,582	0.002 3.27	0.01	5.171	0.023	147.5	1.1	0.0557	0.0002	5,430	25	4,698	635	149.5	1.1
UAA6	ALV-3891-1646-004-004*	Gregg	1,180	3,833	0.008 9.60	0.04	5.648	0.024	144.8	3.0	0.1530	0.0007	15,618	92	14,830	753	151.0	3.2
UAL14	ALV-3891-1646-004-004*	Gregg	1,180	4,921	0.004 12.04	0.05	1.496	0.015	144.8	1.1	0.1495	0.0007	15,242	75	15,071	182	151.1	1.1
UAB16	ALV-3891-1725-005-007*	Gregg	1,222	3,719	0.002 18.84	0.09	14,614	0.064	135.5	1.1	0.3095	0.0015	34,517	208	32,034	2,328	148.4	1.5
UAB17	ALV-3891-1725-005-007*	Gregg	1,222	3,728	0.002 18.31	0.09	2,848	0.013	136.4	1.1	0.3001	0.0015	33,269	197	32,783	510	149.7	1.2
UAB18	ALV-3891-1725-005-007*	Gregg	1,222	4,039	0.003 19.81	0.10	1.817	0.008	139.6	1.1	0.2996	0.0015	33,093	195	32,805	337	153.2	1.2
UAB20	ALV-3891-1725-005-007*	Gregg	1,222	3,852	0.002 18.88	0.09	2,430	0.011	135.2	1.0	0.2995	0.0014	33,232	194	32,829	435	148.3	0.2
UAL10	ALV-3891-1725-005-007	Gregg	1,222	3,734	0.002 18.38	0.08	3,722	0.018	143.5	1.1	0.3008	0.0013	33,108	172	32,455	657	157.3	1.2
UAJ09	ALV-3891-1758-006-003*	Gregg	1,221	3,665	0.002 6.92	0.03	0.797	0.008	140.7	1.1	0.1153	0.0006	11,612	61	11,492	131	145.4	1.1
UAJ05	ALV-3891-1758-006-006*	Gregg	1,221	3,676	0.002 7.02	0.03	5,229	0.023	140.5	1.3	0.1167	0.0005	11,764	57	10,995	721	144.9	1.3
UAJ07	ALV-3891-1758-006-007*	Gregg	1,221	4,058	0.002 9.42	0.04	0.785	0.006	143.4	1.1	0.1419	0.0006	14,428	71	14,319	127	149.3	1.1

Table 1. Continued.

Lab ID	Database ID	Smt.	Depth (m)	²³⁸ U (ppm)	²³⁰ Th (ppt)	²³² Th (ppb)	$\frac{^{230}\text{Th}}{^{238}\text{U}}$ activity	δ^{234} $\frac{U_{\text{mean}}}{\%_{\text{C}_0}}$	Raw age (yrs)	Corr age (yrs)	δ^{234} $\frac{U_{\text{initial}}}{\%_{\text{C}_0}}$								
UAG02	ALV-3904-KEL-201/202 SS02*	Kelvin	1,670	3.345	0.001	18.91	0.08	0.432	1.049	132.6	1.3	0.3455	0.0015	39,432	212	39,338	228	148.2	1.4
UAG04	ALV-3904-KEL-201/202 SS03*	Kelvin	1,670	2.432	0.001	13.79	0.06	0.437	1.093	131.6	1.1	0.3464	0.0015	39,610	212	39,483	242	147.1	1.3
UAF16	ALV-3883-1248-003-003 S*	Manning	1,524	4.632	0.002	0.11	0.00	0.171	0.006	148.9	1.2	0.0014	0.0000	135	1	118	15	148.9	1.2
UAA7	ALV-3883-1248-003-004*	Manning	1,524	3.531	0.008	22.56	0.10	5.145	0.022	129.4	3.0	0.3903	0.0019	45,895	318	44,859	1,055	146.9	3.5
UAA1	ALV-3883-1346-004-003*	Manning	1,506	3.836	0.008	26.35	0.11	8.752	0.037	127.1	3.0	0.4198	0.0020	50,383	352	48,700	1,662	145.9	3.5
UAE04	ALV-3890-1235-001-002	Manning	2,004	3.522	0.002	20.52	0.09	1.019	0.004	139.2	5.0	0.3559	0.0015	40,571	309	40,361	366	156.0	5.6
UAH02	ALV-3890-1235-001-003*	Manning	2,004	4.743	0.003	37.70	0.18	4.342	0.021	122.2	1.2	0.4856	0.0023	61,171	394	60,383	861	144.9	1.4
UAG14	ALV-3890-1330-002-003	Manning	1,886	2.951	0.002	23.73	0.10	9.609	0.442	143.6	1.2	0.4914	0.0022	60,488	367	57,920	2,496	169.1	1.8
UAG05	ALV-3890-1330-002-004*	Manning	1,886	4.162	0.003	11.38	0.05	4.537	0.484	143.4	1.1	0.1670	0.0007	17,187	85	16,594	577	150.3	1.2
UAG07	ALV-3890-1330-002-005	Manning	1,886	2.796	0.001	39.20	0.17	2.000	0.533	115.7	1.2	0.8567	0.0038	152,707	1,483	151,351	1,957	177.4	2.1
UAE19	ALV-3890-1330-002-006	Manning	1,886	3.161	0.002	43.74	0.19	1.225	0.005	117.6	1.2	0.8456	0.0038	147,988	1,410	147,233	1,566	178.3	1.9
UAG06	ALV-3890-1330-002-007*	Manning	1,886	3.640	0.002	9.52	0.04	1.567	0.580	142.2	1.1	0.1597	0.0007	16,399	79	16,164	242	148.8	1.2
UAG20	ALV-3890-1330-002-008	Manning	1,886	3.806	0.002	10.33	0.05	3.767	0.500	150.1	1.2	0.1659	0.0007	16,955	84	16,420	523	157.2	1.3
UAE16	ALV-3890-1407-003-001*	Manning	1,778	3.361	0.002	6.84	0.03	1.888	0.008	144.8	1.1	0.1244	0.0006	12,528	65	12,222	304	149.9	1.1
UAG12	ALV-3890-1407-003-003*	Manning	1,778	3.488	0.002	9.18	0.04	0.866	0.775	145.9	1.1	0.1609	0.0007	16,467	81	16,331	155	152.8	1.2
UAG13	ALV-3890-1407-003-003*	Manning	1,778	3.579	0.002	9.42	0.04	2.138	0.564	143.2	1.1	0.1608	0.0007	16,505	82	16,181	326	149.9	1.2
UAF17	ALV-3890-1642-005-B6 E	Manning	1,487	4.113	0.003	19.43	0.08	3.044	0.022	149.1	1.2	0.2887	0.0013	31,392	164	30,934	474	162.7	1.3
UAK04	ALV-3890-1643-005-0002 lower	Manning	1,487	3.436	0.002	9.99	0.04	0.753	0.017	150.6	1.1	0.1777	0.0008	18,254	89	18,127	152	158.5	1.2
UAK03	ALV-3890-1643-005-0002 upper	Manning	1,487	3.968	0.002	11.10	0.05	1.185	0.014	149.4	1.0	0.1709	0.0007	17,521	85	17,350	187	156.9	1.1
UAJ06	ALV-3890-1643-005-001*	Manning	1,487	3.950	0.002	9.60	0.04	1.900	0.014	132.6	1.1	0.1485	0.0006	15,301	74	15,028	275	138.3	1.2
UAL06	ALV-3890-1643-005-003	Manning	1,487	3.459	0.002	9.48	0.04	0.563	0.015	148.5	1.1	0.1675	0.0007	17,158	83	17,064	123	155.8	1.2
UAE15	ALV-3890-1643-005-004*	Manning	1,487	3.718	0.002	29.11	0.13	0.438	0.002	128.8	1.2	0.4784	0.0022	59,471	365	59,360	377	152.4	1.4
UAE17	ALV-3890-1643-005-005*	Manning	1,487	3.429	0.001	4.06	0.02	0.436	0.002	135.5	1.1	0.0724	0.0003	7,187	35	7,120	74	138.3	1.1
UAJ02	ALV-3890-1643-005-006	Manning	1,487	3.282	0.002	25.57	0.11	1.242	0.011	132.6	1.1	0.4759	0.0021	58,796	344	58,472	462	156.4	1.4
UAF15	ALV-3890-1643-005-B4 F*	Manning	1,487	4.073	0.002	0.17	0.00	0.362	0.006	143.4	1.1	0.0026	0.0000	248	2	207	35	143.5	1.1
UAE05	ALV-3890-1718-006-001*	Manning	1,421	3.267	0.004	2.36	0.01	2.132	0.009	149.6	5.0	0.0441	0.0002	4,272	28	39,44	304	151.3	5.1

Table 1. Continued.

Lab ID	Database ID	Smt.	Depth (m)	²³⁸ U (ppm)	²³⁰ Th (ppt)	²³² Th (ppb)	$\frac{^{230}\text{Th}}{^{238}\text{U}}$ (mean %C)	$\frac{^{230}\text{Th}}{^{238}\text{U}}$ activity	Raw age (yrs)	Corr age (yrs)	$\delta^{234}\text{U}$ (‰)								
UA007	ALV-3890-1742-007-001*	Manning	1,381	4.292	0.002	11.14	0.05	2.975	0.013	146.0	1.1	0.1586	0.0007	16,215	78	15,825	386	152.7	1.2
UA020	ALV-3890-1742-007-002	Manning	1,381	3.039	0.002	8.05	0.03	0.987	0.007	148.4	1.1	0.1619	0.0007	16,536	80	16,351	196	155.4	1.2
UA008	ALV-3892-1315-001-002*	Manning	1,713	3.143	0.001	16.86	0.07	0.405	0.002	134.9	4.0	0.3278	0.0014	36,951	251	36,860	263	149.7	4.5
UA009	ALV-3892-1315-001-003*	Manning	1,713	3.829	0.002	10.08	0.04	2.548	0.011	143.5	1.2	0.1609	0.0007	16,509	79	16,133	374	150.2	1.2
UA016	ALV-3892-1315-001-003	Manning	1,713	4.031	0.002	10.28	0.05	0.694	0.017	148.7	1.1	0.1558	0.0007	15,868	80	15,773	121	155.5	1.1
UA005	ALV-3892-1315-001-006	Manning	1,713	3.284	0.002	16.82	0.07	1.185	0.014	140.9	1.1	0.3129	0.0014	34,757	181	34,512	297	155.3	1.2
UA011	ALV-3892-1315-001-007*	Manning	1,713	6.668	0.004	27.07	0.12	8.491	0.036	137.2	1.2	0.2481	0.0011	26,736	139	25,977	746	147.6	1.3
UA012	ALV-3892-1315-001-007*	Manning	1,713	6.683	0.005	26.86	0.12	9.705	0.043	129.4	4.0	0.2456	0.0011	26,651	177	25,781	856	139.2	4.3
UA013	ALV-3892-1315-001-007*	Manning	1,713	6.520	0.003	26.34	0.11	8.511	0.036	136.0	1.0	0.2469	0.0011	26,625	137	25,848	755	146.4	1.1
UA014	ALV-3892-1315-001-007*	Manning	1,713	6.607	0.003	26.46	0.13	8.492	0.037	134.1	1.0	0.2447	0.0012	26,410	150	25,644	755	144.2	1.2
UA015	ALV-3892-1315-001-007*	Manning	1,713	6.409	0.003	25.92	0.12	8.325	0.036	134.5	1.1	0.2471	0.0011	26,690	146	25,915	763	144.7	1.2
UA017	ALV-3892-1315-001-007*	Manning	1,713	6.695	0.003	26.82	0.12	10.268	0.044	135.0	1.0	0.2475	0.0011	26,393	132	25,444	922	145.0	1.2
UA015	ALV-3892-1315-001-007*	Manning	1,713	4.540	0.002	17.65	0.08	3.234	0.019	136.0	1.0	0.2375	0.0010	25,496	128	25,073	431	146.0	1.2
UA003	ALV-3892-1315-001-008*	Manning	1,713	3.516	0.002	9.05	0.04	1.396	0.006	142.1	4.0	0.1572	0.0007	16,123	99	15,906	232	148.6	4.2
UA016	ALV-3892-1315-001-008*	Manning	1,713	3.525	0.002	9.15	0.04	0.756	0.007	142.4	1.1	0.1586	0.0007	16,268	78	16,145	142	149.1	1.1
UA001	ALV-3892-1315-001-010*	Manning	1,713	4.712	0.002	21.83	0.09	0.535	0.002	128.1	4.0	0.2831	0.0012	31,372	207	31,296	218	139.9	4.4
UA007	ALV-3892-1315-001-B4-SS1	Manning	1,713	3.120	0.002	9.28	0.04	0.905	0.012	149.2	1.1	0.1817	0.0008	18,726	91	18,557	187	157.2	1.1
UA008	ALV-3892-1315-001-B4-SS2	Manning	1,713	3.862	0.002	8.50	0.04	0.713	0.014	149.4	1.1	0.1344	0.0006	13,549	64	13,446	119	155.2	1.1
UA009	ALV-3892-1315-001-B4-SS3*	Manning	1,713	3.622	0.002	9.41	0.04	0.684	0.008	142.8	1.2	0.1587	0.0007	16,273	81	16,164	133	149.5	1.2
UA007	ALV-3892-1711-006-002	Manning	1,548	3.181	0.003	24.49	0.11	2.157	0.009	136.8	4.1	0.4704	0.0022	57,607	450	57,068	685	160.7	4.8
UA002	ALV-3892-1711-006-004*	Manning	1,548	3.687	0.003	21.08	0.09	0.929	0.004	134.3	4.0	0.3493	0.0016	39,880	278	39,704	323	150.3	4.5
UA004	ALV-3892-1711-006-006	Manning	1,548	3.331	0.003	25.63	0.11	1.544	0.007	135.0	4.0	0.4701	0.0021	57,686	446	57,313	569	158.7	4.8
UA010	ALV-3892-1711-006-008	Manning	1,548	3.384	0.002	19.37	0.09	0.808	0.003	140.2	4.0	0.3496	0.0016	36,951	256	36,860	318	156.7	4.5
UA006	ALV-3892-1711-006-010*	Manning	1,548	3.250	0.003	18.64	0.08	0.943	0.004	133.0	4.0	0.3505	0.0016	40,099	282	39,896	340	148.9	4.5
From the fallen gorgonian coral																			
UA001a	ALV-3892-1421-002-001-05*	Manning	1,657	4.263	0.003	26.61	0.11	1.502	0.007	130.4	5.0	0.3814	0.0017	44,549	350	44,284	430	147.8	5.7

Table 1. Continued.

Lab ID	Database ID	Smt.	Depth (m)	238U (ppm)	230Th (ppt)	232Th (ppb)	$\delta^{234}\text{U}$ $\text{U}_{\text{mean}}/\text{‰}$	$(^{230}\text{Th}/^{238}\text{U})$ activity	Raw age (yrs)	Corr age (yrs)	$\delta^{234}\text{U}$ $\text{U}_{\text{initial}}/\text{‰}$								
UAD001	ALV-3892-1421-002-001-06*	Manning	1,657	3,246	0.002	19.64	0.18	0.500	0.024	130.0	4.0	0.3697	0.0033	42,918	509	42,799	519	146.8	4.5
UAD002	ALV-3892-1421-002-001-07*	Manning	1,657	4,070	0.002	18.22	0.12	0.492	0.015	130.6	4.0	0.2735	0.0018	30,074	265	29,991	275	142.1	4.4
UAD003	ALV-3892-1421-002-001-08*	Manning	1,657	2,815	0.002	16.99	0.16	0.296	0.023	133.4	4.0	0.3688	0.0035	42,624	532	42,541	536	150.4	4.5
UAD004	ALV-3892-1421-002-001-09*	Manning	1,657	4,419	0.003	27.16	0.22	3.412	0.032	126.1	4.0	0.3756	0.0030	43,943	475	43,374	725	142.5	4.6
UAD005	ALV-3892-1421-002-001-10*	Manning	1,657	3,564	0.002	21.88	0.10	0.468	0.002	135.2	4.0	0.3752	0.0017	43,432	307	43,329	319	152.9	4.5
UAD006	ALV-3892-1421-002-001-11	Manning	1,657	3,486	0.002	21.45	0.09	0.875	0.004	136.2	4.0	0.3761	0.0016	43,509	304	43,321	351	154.0	4.5
UAD007	ALV-3892-1421-002-001-12*	Manning	1,657	4,442	0.002	27.64	0.12	2.253	0.010	131.6	4.0	0.3803	0.0017	44,332	314	43,956	479	149.0	4.6
UAD008	ALV-3892-1421-002-001-13*	Manning	1,657	4,394	0.002	27.20	0.12	1.731	0.007	135.2	4.0	0.3782	0.0017	43,857	308	43,565	415	152.9	4.5
UAD009	ALV-3892-1421-002-001-14*	Manning	1,657	3,796	0.001	23.53	0.11	0.529	0.002	134.1	4.0	0.3787	0.0018	43,982	323	43,873	336	151.8	4.5
UAD010	ALV-3892-1421-002-001-15*	Manning	1,657	3,429	0.001	21.16	0.10	0.874	0.004	127.6	4.0	0.3771	0.0017	44,075	319	43,881	366	144.5	4.5
UAD011	ALV-3892-1421-002-001-16*	Manning	1,657	3,577	0.002	22.33	0.16	1.390	0.007	132.2	4.0	0.3814	0.0027	44,464	436	44,174	515	149.8	4.6
UAD012	ALV-3892-1421-002-001-17*	Manning	1,657	3,506	0.002	22.97	0.25	0.562	0.004	134.3	4.0	0.4003	0.0044	47,078	681	46,950	689	153.4	4.6
UAD013	ALV-3892-1421-002-001-18*	Manning	1,657	3,460	0.002	21.40	0.09	0.631	0.003	123.9	4.0	0.3779	0.0016	44,385	313	44,243	338	140.4	4.6
UAD015	ALV-3892-1421-002-001-20*	Manning	1,657	3,091	0.002	23.24	0.10	1.233	0.005	139.9	4.0	0.4594	0.0020	55,662	417	55,334	519	163.6	4.7
UAE02	ALV-3892-1421-002-001-20*	Manning	1,657	3,214	0.003	24.30	0.11	0.705	0.003	130.3	5.0	0.4620	0.0021	56,719	482	56,529	509	152.9	5.9
UAD20	ALV-3892-1421-002-001-25*	Manning	1,657	3,730	0.002	31.48	0.14	1.696	0.007	126.7	4.0	0.5156	0.0022	65,900	518	65,485	649	152.4	4.8
UAD14	ALV-3892-1421-002-001-19 Go	Manning	1,657	1,151	0.000	0.78	0.00	0.131	0.001	142.4	4.3	0.3172	0.0018	35,270	292	34,686	636	157.1	4.8
UAD16	ALV-3892-1421-002-001-21 Go*	Manning	1,657	0,094	0.000	0.58	0.01	0.660	0.003	135.5	4.1	0.3813	0.0082	44,287	1,192	39,292	4,630	151.4	5.0
UAD17	ALV-3892-1421-002-001-22 Go	Manning	1,657	1,186	0.000	1.00	0.02	0.418	0.002	161.0	4.1	0.3294	0.0081	36,146	1,061	34,673	1,742	177.5	4.6
UAD18	ALV-3892-1421-002-001-23 Go	Manning	1,657	1,154	0.000	0.82	0.02	0.049	0.001	154.6	4.0	0.3262	0.0071	35,975	939	35,757	956	171.1	4.5
UAD19	ALV-3892-1421-002-001-24 Go	Manning	1,657	1,146	0.000	0.98	0.06	0.083	0.001	162.2	4.1	0.4109	0.0269	47,109	3,887	46,691	3,867	185.1	5.1
UAE11	ALV-3884-1411-002-104*	Muir	2,228	3,199	0.002	8.28	0.04	1.659	0.007	142.6	1.1	0.1581	0.0007	16,218	79	15,925	296	149.2	1.2
UAF08	ALV-3884-1531-002-013*	Muir	2,228	3,383	0.002	8.42	0.04	0.339	0.011	140.2	1.1	0.1521	0.0007	15,586	75	15,530	92	146.5	1.1
UAJ17	ALV-3884-1531-003-008*	Muir	2,141	3,700	0.003	9.24	0.04	2.201	0.016	145.5	1.2	0.1526	0.0007	15,571	77	15,237	333	151.9	1.3
UAE13	ALV-3884-1531-003-011*	Muir	2,141	2,859	0.002	46.82	0.20	3.189	0.014	111.0	5.0	1.0008	0.0043	229,510	5,302	225,285	6,417	209.9	10.1
UAJ19	ALV-3884-1638-004-014*	Muir	2,084	3,836	0.003	9.95	0.04	0.927	0.008	140.0	1.1	0.1584	0.0007	16,288	80	16,149	157	146.6	1.2

Table 1. Continued.

Lab ID	Database ID	Smt.	Depth (m)	238U (ppm)	230Th (ppt)	232Th (ppb)	δ^{234} U _{mean} ‰	$(^{230}\text{Th}/^{238}\text{U})$ activity	Raw age (yrs)	Corr age (yrs)	δ^{234} U _{initial} ‰								
UAE12	ALV-3884-1638-004-210*	Muir	2,084	3.286	0.002	8.16	0.04	0.422	0.002	141.7	1.2	0.1518	0.0007	75	15,458	103	148.0	1.2	
UA102	ALV-3885-1239-001-002*	Muir	2,027	3.507	0.002	9.99	0.05	0.190	0.042	145.2	1.1	0.1741	0.0009	17,945	100	16,462	1,369	152.2	1.3
UAG15	ALV-3885-1239-001-004*	Muir	2,027	3.416	0.002	9.10	0.04	1.602	0.625	142.2	1.1	0.1627	0.0007	16,733	82	16,476	263	149.0	1.2
UAE10	ALV-3885-1239-001-007	Muir	2,027	3.129	0.002	8.47	0.04	3.092	0.013	146.5	1.1	0.1654	0.0007	16,963	82	16,405	544	153.4	1.2
UAO17	ALV-3885-1239-001-007	Muir	2,027	3.135	0.002	7.99	0.04	0.694	0.013	146.7	1.1	0.1558	0.0007	15,901	78	15,780	141	153.4	1.1
UAG08	ALV-3885-1239-001-011*	Muir	2,027	2.289	0.002	5.99	0.03	0.672	0.989	140.6	1.1	0.1599	0.0007	16,438	80	16,277	176	147.2	1.2
UA103	ALV-3885-1239-001-012*	Muir	2,027	3.087	0.002	8.16	0.04	1.793	0.010	142.1	1.1	0.1615	0.0008	16,598	90	16,268	333	148.8	1.2
UAO18	ALV-3885-1239-001-012	Muir	2,027	3.316	0.002	8.43	0.04	0.882	0.013	150.6	1.1	0.1553	0.0007	15,781	77	15,637	160	157.4	1.1
UAE06	ALV-3885-1239-001-014*	Muir	2,027	4.829	0.002	12.63	0.05	1.116	0.005	142.4	1.1	0.1598	0.0007	16,401	79	16,268	151	149.1	1.2
UAG11	ALV-3885-1239-001-015*	Muir	2,027	3.384	0.002	8.81	0.04	0.735	1.214	141.6	1.1	0.1591	0.0007	16,343	81	16,223	141	148.3	1.2
UAE20	ALV-3885-1325-002-034*	Muir	1,986	3.262	0.001	22.12	0.10	1.705	0.007	130.8	1.1	0.4143	0.0019	49,345	284	48,939	484	150.2	1.3
UAF06	ALV-3885-1325-002-039*	Muir	1,986	3.695	0.002	24.73	0.11	1.184	0.012	126.0	1.2	0.4089	0.0018	48,815	275	48,572	359	144.6	1.3
UAF09	ALV-3885-1420-003-003*	Muir	1,929	3.634	0.002	27.95	0.12	1.203	0.009	121.6	1.1	0.4699	0.0020	58,615	343	58,339	431	143.4	1.3
UAG19	ALV-3885-1452-004-001*	Muir	1,878	3.465	0.001	28.25	0.12	4.744	0.438	127.0	1.2	0.4981	0.0022	62,883	378	61,746	1,168	151.2	1.5
UAE14	ALV-3885-1452-004-003*	Muir	1,878	3.420	0.002	26.56	0.12	1.651	0.007	126.6	1.2	0.4745	0.0022	59,005	365	58,593	538	149.4	1.4
UA101	ALV-3885-1452-004-007*	Muir	1,878	3.573	0.002	24.65	0.11	0.987	0.010	128.1	1.2	0.4215	0.0018	50,574	286	50,351	355	147.7	1.3
UAF03	ALV-3885-1452-004-010*	Muir	1,878	3.353	0.002	26.60	0.11	1.905	0.014	127.9	1.1	0.4847	0.0021	60,583	359	60,113	578	151.6	1.4
UAG17	ALV-3885-1520-005-006	Muir	1,821	4.437	0.002	63.94	0.30	2.420	0.531	100.6	1.2	0.8805	0.0042	167,947	1,899	166,726	2,204	161.2	2.1
UAG10	ALV-3885-1520-005-007-lower	Muir	1,821	1.138	0.002	16.31	0.07	0.501	1.405	103.0	1.2	0.8761	0.0041	165,089	1,831	164,118	2,029	163.9	2.1
UAG09	ALV-3885-1520-005-007-upper	Muir	1,821	6.698	0.004	95.63	0.42	2.488	0.528	106.4	1.1	0.8723	0.0038	162,169	1,645	161,364	1,793	167.9	2.0
UAH06	ALV-3885-1520-005-008*	Muir	1,821	3.848	0.001	26.16	0.12	1.448	0.008	128.0	1.1	0.4153	0.0019	49,656	289	49,359	405	147.1	1.3
UAG18	ALV-3885-1520-005-012	Muir	1,821	4.580	0.002	66.03	0.30	6.045	0.448	101.0	1.2	0.8808	0.0040	167,944	1,823	165,097	3,290	161.1	2.4
UAE18	ALV-3885-1520-005-014	Muir	1,821	4.587	0.002	65.27	0.29	2.796	0.012	100.5	1.2	0.8693	0.0039	163,232	1,719	161,878	2,132	158.8	2.1
UAG16	ALV-3885-1739-007-003	Muir	1,791	2.693	0.002	42.33	0.19	3.676	0.477	96.9	1.1	0.9605	0.0042	212,243	2,896	207,902	5,063	174.5	3.2
UA120	ALV-3887-1324-002-002*	Muir	2,546	4.330	0.002	8.82	0.04	0.810	0.007	142.9	1.2	0.1244	0.0006	12,553	61	12,449	117	148.1	1.2
UAJ20	ALV-3887-1324-002-005*	Muir	2,546	4.596	0.003	9.33	0.04	0.572	0.008	140.9	1.1	0.1241	0.0006	12,545	61	12,475	91	145.9	1.2

Table 1. Continued.

Lab ID	Database ID	Smt.	Depth 238U (m)	²³⁸ Th (ppt)	²³² Th (ppb)	²³⁰ Th (pmol)	δ^{234} U _{mean} ‰	$\frac{(^{230}\text{Th}/^{238}\text{U})}{\text{activity}}$	Raw age (yrs)	Corr age (yrs)	δ^{234} U _{initial} ‰								
UA116	ALV-3887-1436-003-003*	Muir	2,441	3,488	0.002	8.65	0.04	0.657	0.010	143.5	1.1	0.1515	0.0007	15,478	76	15,370	129	149.8	1.2
UA106	ALV-3887-1436-003-006*	Muir	2,441	3,750	0.001	39.46	0.17	2.076	0.010	116.6	1.2	0.6430	0.0028	91,822	637	91,181	882	150.9	1.6
UAF05	ALV-3887-1436-003-007*	Muir	2,441	3,296	0.002	32.52	0.14	1.355	0.010	121.5	1.1	0.6028	0.0026	82,722	552	82,297	681	153.4	1.5
UAF04	ALV-3887-1436-003-010*	Muir	2,441	3,665	0.002	37.74	0.16	0.982	0.010	118.1	1.1	0.6292	0.0027	88,626	605	88,325	664	151.6	1.5
UA119	ALV-3887-1436-003-011*	Muir	2,441	3,366	0.002	35.36	0.15	4.363	0.021	117.6	1.2	0.6417	0.0028	91,400	641	89,942	1,553	151.6	1.7
UAJ04	ALV-3887-1549-004-002*	Muir	2,372	3,755	0.002	9.30	0.04	0.474	0.004	142.1	1.1	0.1513	0.0007	15,475	75	15,402	102	148.4	1.2
UAK02	ALV-3887-1549-004-004*	Muir	2,372	3,470	0.002	9.01	0.04	0.539	0.006	143.3	1.1	0.1586	0.0007	16,258	77	16,168	116	150.0	1.1
UA114	ALV-3887-1549-004-005*	Muir	2,372	3,943	0.003	10.12	0.04	0.918	0.006	140.2	1.3	0.1569	0.0007	16,113	80	15,980	152	146.6	1.3
UAF13	ALV-3887-1549-004-006*	Muir	2,372	3,812	0.002	9.70	0.04	0.925	0.010	139.2	1.1	0.1556	0.0007	15,986	77	15,853	150	145.6	1.2
UAL19	ALV-3887-1549-004-006*	Muir	2,372	3,922	0.005	10.07	0.04	1.609	0.009	136.3	1.3	0.1569	0.0007	16,181	81	15,947	242	142.6	1.4
UAF11	ALV-3887-1549-004-007*	Muir	2,372	4,039	0.002	8.36	0.04	0.584	0.008	139.6	1.1	0.1265	0.0006	12,822	61	12,744	96	144.7	1.1
UAF12	ALV-3887-1549-004-008	Muir	2,372	4,282	0.002	10.55	0.05	0.592	0.009	148.3	1.0	0.1506	0.0007	15,303	73	15,227	103	154.8	1.1
UA117	ALV-3887-1549-004-009*	Muir	2,372	3,360	0.002	6.96	0.03	0.159	0.007	143.3	1.1	0.1266	0.0006	12,780	62	12,752	67	148.5	1.2
UAF02	ALV-3887-1549-004-012*	Muir	2,372	3,286	0.002	6.76	0.03	0.561	0.012	142.5	1.1	0.1258	0.0006	12,707	61	12,616	107	147.7	1.1
UAA5	ALV-3887-1549-004-014*	Muir	2,372	3,651	0.007	8.99	0.04	0.524	0.002	144.6	3.0	0.1505	0.0007	15,348	90	15,269	118	151.0	3.1
UAL09	ALV-3887-1549-004-014*	Muir	2,372	3,644	0.002	8.99	0.04	0.327	0.007	147.3	1.1	0.1508	0.0007	15,341	74	15,289	89	153.8	1.1
UAA3	ALV-3887-1652-005-006*	Muir	2,265	3,637	0.007	9.82	0.04	6.892	0.030	143.0	3.0	0.1649	0.0008	16,960	101	15,934	969	149.6	3.2
UAL12	ALV-3887-1652-005-006*	Muir	2,265	3,480	0.001	7.16	0.03	0.384	0.005	142.4	1.1	0.1258	0.0005	12,705	59	12,643	84	147.6	1.1
UAF10	ALV-3887-1652-005-013*	Muir	2,265	3,882	0.002	9.94	0.04	0.719	0.008	141.4	1.1	0.1564	0.0007	16,042	77	15,939	125	147.9	1.2
UAF14	ALV-3887-1652-005-018*	Muir	2,265	4,071	0.003	0.34	0.00	0.622	0.014	148.9	1.2	0.0051	0.0000	489	4	418	61	149.1	1.2
UAM15	ALV-3889-1311-001-001*	Muir	1,719	3,977	0.002	11.34	0.05	1.575	0.008	132.5	1.1	0.1742	0.0008	18,181	89	17,950	242	139.4	1.2
UAJ12	ALV-3889-1311-001-002*	Muir	1,719	4,253	0.002	17.20	0.07	2.689	0.021	137.2	1.1	0.2471	0.0011	26,622	133	26,228	407	147.8	1.2
UAM09	ALV-3889-1311-001-003	Muir	1,719	3,332	0.002	12.44	0.05	4.711	0.021	139.3	1.1	0.2282	0.0010	24,293	122	23,438	832	148.9	1.3
UA118	ALV-3889-1311-001-004	Muir	1,719	3,193	0.002	8.74	0.04	1.231	0.013	150.3	1.1	0.1673	0.0007	17,103	82	16,884	229	157.6	1.1
UAM12	ALV-3889-1311-001-005*	Muir	1,719	3,257	0.002	12.88	0.06	3.702	0.017	135.0	1.1	0.2417	0.0010	26,020	131	25,317	693	145.0	1.3
UAA4	ALV-3889-1311-001-006*	Muir	1,719	3,262	0.007	14.23	0.06	3.177	0.014	134.0	3.0	0.2665	0.0013	29,097	183	28,501	607	145.3	3.3

Table 1. Continued.

Lab ID	Database ID	Smt.	Depth (m)	238U (ppm)	230Th (ppt)	232Th (ppb)	$\delta^{234}\text{U}_{\text{perm}}\%$	$(^{230}\text{Th}/^{238}\text{U})$ activity	Raw age (yrs)	Corr age (yrs)	$\delta^{234}\text{U}_{\text{initial}}\%$								
UAL13	ALV-3889-1311-001-006*	Muir	1,719	3.316	0.002	14.49	0.06	1.011	0.019	135.4	1.2	0.2671	0.0012	29,121	150	28,923	243	146.9	1.3
UAL15	ALV-3889-1311-001-007	Muir	1,719	3.530	0.002	9.23	0.04	0.709	0.010	147.9	1.1	0.1598	0.0007	16,319	78	16,204	136	154.8	1.1
UAMI0	ALV-3889-1311-001-008*	Muir	1,719	3.852	0.002	18.06	0.08	1.649	0.009	139.6	1.1	0.2866	0.0012	31,434	161	31,153	316	152.4	1.2
UAMI1	ALV-3889-1311-001-008*	Muir	1,719	3.711	0.002	16.78	0.07	9.407	0.041	135.5	1.1	0.2763	0.0012	30,275	155	28,660	1,540	146.9	1.3
UAL20	ALV-3889-1326-002-B7*	Muir	1,723	3.048	0.002	47.76	0.21	2.142	0.011	82.1	1.2	0.9575	0.0042	221,140	3,172	218,494	4,005	152.3	2.7
UAA2	ALV-3889-1353-003-001*	Muir	1,714	3.442	0.007	11.58	0.05	21.778	0.095	145.2	3.0	0.2056	0.0010	21,518	134	18,006	2,975	152.8	3.5
UAL08	ALV-3889-1353-003-001*	Muir	1,714	3.350	0.002	9.46	0.04	5.420	0.026	146.0	1.1	0.1725	0.0008	17,752	87	16,835	874	153.1	1.2
UAA8	ALV-3889-1526-006-001	Muir	1,620	3.890	0.008	55.53	0.24	26.943	0.115	102.2	3.0	0.8723	0.0042	163,812	2,140	150,328	13,015	156.3	7.6
UAE08	ALV-3889-1526-006-001	Muir	1,620	4.022	0.002	56.80	0.24	3.052	0.013	97.9	1.1	0.8629	0.0037	161,549	1,619	159,899	2,249	153.8	1.9
UAE03	ALV-3889-1526-006-B2	Muir	1,620	4.936	0.003	59.92	0.26	4.284	0.018	120.5	5.0	0.7419	0.0032	115,159	1,340	113,946	1,754	166.2	7.0
UAF01	ALV-3890-1643-005-009	Muir	1,487	3.318	0.005	16.75	0.08	2.132	0.041	143.3	1.2	0.3085	0.0015	34,105	197	33,694	445	157.6	1.4

Table 2. Summary of U-series dated scleractinian corals. In all, 159 measurements were made on 127 coral individuals yielding 99 separate reliable ages. All samples in this table are *Desmophyllum dianthus* except two *Caryophyllia* and one *Solenosmilia* from Gregg and one *Solenosmilia* and two *Enallopsammia* from Manning as marked in Table 1.

Seamount	Measurements	Individuals	Reliable ages
Bear	3	3	1
Gregg	21	15	14
Kelvin	2	2	2
Manning	65	55	37
Muir	68	52	45
Total	159	127	99

al., 1996). The three oldest population peaks occur close to the times of three Heinrich events, each of which originated in the Hudson Straits (Hemming, 2004). The youngest population peak occurs during the Younger Dryas, which is thought to have a similar water-mass configuration to the Heinrich events (Boyle and Keigwin, 1987).

Changes in ocean circulation appear to have a marked effect on the populations of *D. dianthus* of the New England Seamounts, but determining the cause of the effect is difficult. The fact that no corals were found with LGM ages suggests that the oceanographic configuration was not well suited to coral recruitment and/or growth. Unfortunately, the notch morphology of the sites that were sampled on Muir prevents us from isolating the effect of the presence of deep southern-source water on *D. dianthus* during the LGM. The presence of the shallower (< 2000 m) northern-sourced water does not appear to have been conducive to abundant coral growth.

Rapid encroachments of an intermediate depth (1700–2000 m) southern-source water mass have been recognized in the NW Atlantic at several times during the deglaciation (Adkins et al., 1998; Robinson et al., 2005). The radiocarbon composition from the skeletons of multiple corals recorded the switch from intermediate depth northern to southern-source waters, and vice versa, indicating that *D. dianthus* thrives in conditions in which the ocean is experiencing rapid climate change. Whether these switches brought about beneficial environmental changes (more nutrients, higher current rates?), or allowed coral larvae to reach Muir and Manning Seamounts is unresolved. To best answer this question we would need to make further collections of *D. dianthus* from deep on Muir Seamount, specifically to a second notch feature that extends to greater depths.

GREGG SEAMOUNT.—The oldest dated corals from Gregg Seamount, are ~15 ka, and corals are present from throughout the rest of the deglaciation. This age distribution contrasts markedly to they pulsing seen at Muir and Manning, although the sample size is small. The difference between distribution patterns at Gregg and Muir/Manning may be controlled by depth or geographic location. The Gregg samples were all collected from ~1200 m, whereas the shallowest samples from Muir or Manning were at 1400 m. An alternative control may be the relative locations of the three seamounts. Gregg is situated farther northwest than Muir and Manning, close to the position of the modern Gulf Stream. The strong currents of the Gulf Stream may be important in controlling larval dispersal or supply of food to coral populations. The position of the Gulf Stream in the past is not well defined, but shifts in its latitude or velocity may have caused the coral populations in the two locations to be different from one another. To test whether the geographic location or the depth range is the most important control on the age distribution, we would need to collect

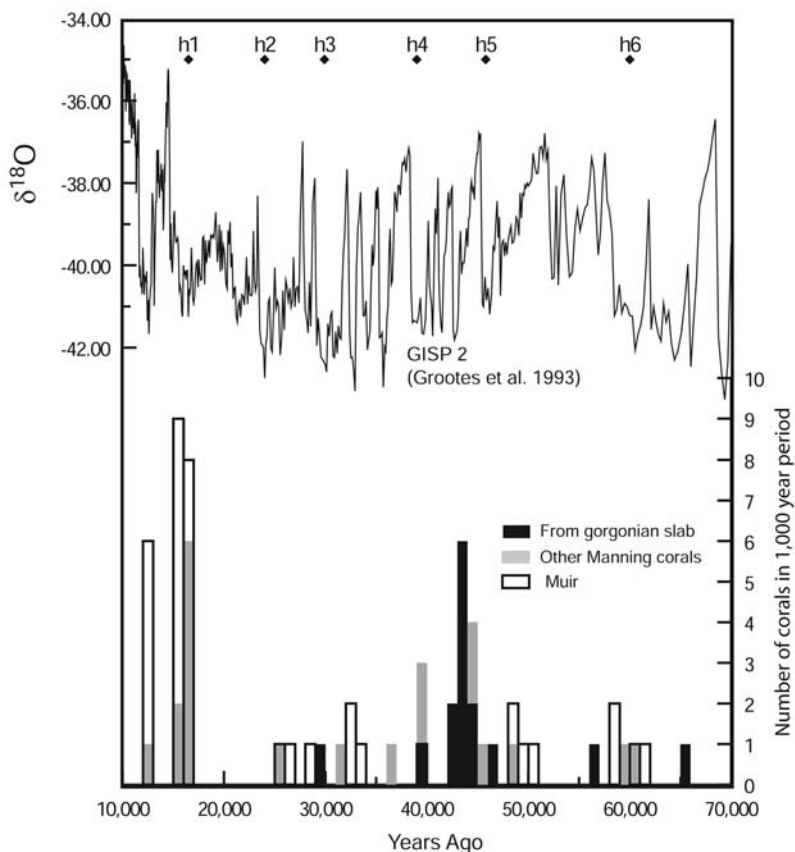


Figure 6. Number of *Desmophyllum dianthus* from Muir (white) and Manning Seamounts. The Manning individuals are divided into those sampled from the build-up pictured in Figure 5 (black) and all other samples (grey). The upper curve is the GISP 2 $\delta^{18}\text{O}$ record from Greenland covering the last glacial period, which lasted from ~ 70 – 10 ka. The glacial was characterized by large climate variations shown by the large oscillations in the $\delta^{18}\text{O}$ signal. In addition, marine records have shown pulses of large quantities of ice-rafted debris during the last deglacial. The last six of these Heinrich events are labeled H1–H6 at ages taken from (Hemming, 2004).

deeper samples from Gregg to compare to the more southerly seamounts. We could also date corals from farther along the seamount chain out towards the Corner Rise Seamounts.

NW AND NE ATLANTIC AGE DISTRIBUTIONS.—Fossil corals have been collected from multiple locations including the Southern Ocean and NE Atlantic (Goldstein et al., 2001; Schröder-Ritzrau et al., 2003; Frank et al., 2004; Dorschel et al., 2005). Only from the east Atlantic have sufficient corals been dated to provide a comparison to the age distributions shown in this paper (Schröder-Ritzrau et al., 2003; Frank et al., 2004; Dorschel et al., 2005). Most of the corals dated from the NE Atlantic are colonial species such as *Lophelia pertusa* (Linnaeus, 1758), however Schroeder-Ritzrau et al. (2005) also present ten ages from solitary corals (*D. dianthus* and *Caryophyllia*). The distribution of corals ages from the east Atlantic does not show the strong tendency towards glacial age corals observed in the NW Atlantic. Indeed, more than 60% of the dated corals (colonial and solitary) are modern or Holocene in age. The corals from the east Atlantic range in latitude from 2°N – 64°N and from < 80 m to

2306 m water depth, spanning a wide range of geographical and oceanographic settings. When this wide distribution is coupled with the number of samples dated, it becomes impossible to make a statistical comparison between the age distributions in the east and west basins of the North Atlantic.

CONCLUSIONS

Fossil deep-sea corals provide an ideal archive for recording conditions in the past ocean as their skeletons record a signature of the water mass in which they lived (Smith et al., 1997; Adkins et al., 1998). More simply, their presence or absence over long time periods can help to resolve questions of the major controls on deep-sea coral distributions. Fossil corals collected from the New England Seamounts on three cruises during 2003–2005 show a distinct depth distribution, with *D. dianthus* abundant down to 2500 m and colonial scleractinian corals abundant to depths of 1800 m. The 2500 m maximum depth of a notch feature on Muir seamount may be the most important control on the depth cut-off of *D. dianthus*. U-series analysis ages of *D. dianthus* individuals indicate that the largest number of corals was alive during the last glacial period. Within this time, on Muir and Manning Seamounts, the population density of *D. dianthus* was pulsed, and these pulses coincided with major ocean circulation changes as recorded by other paleoceanographic proxies (Boyle and Keigwin, 1987). *Desmophyllum dianthus* appears to thrive in conditions during which the ocean is experiencing rapid climate change. On Gregg Seamount, the population distribution is more continuous. The difference between Gregg compared to Muir and Manning may be caused either by sample depth (all Gregg samples were shallower than the other Seamounts) or position (Gregg is to the north). We could put tighter constraints on the links between coral distribution and oceanographic change by making collections at greater depths, and exploring different topographic morphologies, from both Gregg and Muir Seamounts.

ACKNOWLEDGMENTS

We gratefully acknowledge the support of The Comer Foundation for Abrupt Climate Change, The Henry Luce Foundation, The American Chemical Society Petroleum Research Fund, NSF Grant Numbers OCE-0096373 and OCE-0095331, and NOAA OE Grant Number A05OAR4601054. We would also like to thank the crew, the science parties, and the DSV ALVIN and ROV HERCULES pilots on RV ATLANTIS cruise AT7-35 and AT8-1, and the DASS05 expedition to the New England Seamounts.

LITERATURE CITED

- Adkins, J. F. and D. S. Scheirer. New England Seamounts 2003: AT7-35 Cruise Report. 2003. 95 p.
- _____, E. A. Boyle, W. B. Curry, and A. Lutringer. 2003. Stable isotopes in deep-sea corals and a new mechanism for "vital effects". *Geochim. Cosmochim. Acta* 67: 1129–1143.
- _____, H. Cheng, E. A. Boyle, E. R. M. Druffel, and R. L. Edwards. 1998. Deep-sea coral evidence for rapid change in ventilation of the deep North Atlantic 15,400 years ago. *Science* 280: 725–728.
- _____, G. M. Henderson, S. L. Wang, S. O'Shea, and F. Mokadem. 2004. Growth rates of the deep-sea scleractinia *Desmophyllum cristagalli* and *Enallopsammia rostrata*. *Earth Planet. Sci. Lett.* 227: 481–490.

- Bard, E., R. G. Fairbanks, B. Hamelin, A. Zindler, and H. Chi Trach. 1991. Uranium-234 anomalies in corals older than 150 000 years. *Geochim. Cosmochim. Acta* 55: 2385–2390.
- Bond, Z. A., A. L. Cohen, S. R. Smith, and W. J. Jenkins. 2005. Growth and composition of high-Mg calcite in the skeleton of a Bermudian gorgonian (*Plexaurella dichotoma*): Potential for paleothermometry. *Geochem. Geophys. Geosyst.* Q08010, doi:10.1029/2005GC000911.
- Boyle, E. A. and L. D. Keigwin. 1987. North Atlantic thermohaline circulation during the past 20 000 years linked to high-latitude surface temperature. *Nature* 330: 35–40.
- Broecker, W., S. L. Peacock, S. Walker, R. F. Weiss, V. Fahrenbach, M. Schroeder, U. Mikolajewicz, C. Heinze, R. Key, T. H. Peng, and S. Rubin. 1998. How much deep water is formed in the Southern Ocean? *J. Geophys. Res.* 103: 15,833–15,843
- Broecker, W. S. 1998. Paleocirculation during the last deglaciation: a bipolar seesaw? *Paleoceanography* 13: 119–121.
- _____ and T. Takahashi. 1966. Calcium carbonate precipitation on the Bahama Banks. *J. Geophys. Res.* 71: 1575–1602.
- Cheng, H., J. F. Adkins, R. L. Edwards, and E. A. Boyle. 2000. U-Th dating of deep-sea corals. *Geochim. Cosmochim. Acta* 64: 2401–2416.
- _____, R. L. Edwards, J. Hoff, C. D. Gallup, D. A. Richards, and Y. Asmeron. 2000. The half-lives of uranium-234 and thorium-230. *Chem. Geol.* 169: 17–33.
- Cohen, A. L., G. D. Layne, S. R. Hart, and P. S. Lobel. 2001. Kinetic control of skeletal Sr/Ca in a symbiotic coral: Implications for the paleotemperature proxy. *Paleoceanography* 16: 20–26.
- Curry, W. B. and D. W. Oppo. 2005. Glacial water mass geometry and the distribution of delta C-13 of Sigma CO2 in the western Atlantic Ocean. *Paleoceanography* 20 PA1017.
- Cutler, K. B., R. L. Edwards, F. W. Taylor, H. Cheng, J. F. Adkins, C. D. Gallup, P. M. Cutler, G. S. Burr, and A. L. Bloom. 2003. Rapid sea-level fall and deep-ocean temperature change since the last interglacial period. *Earth Planet. Sci. Lett.* 206: 253–271.
- Dorschel, B., D. Hebbeln, A. Rüggeberg, W. C. Dullo, and A. Freiwald. 2005. Growth and erosion of a cold-water coral covered carbonate mound in the Northeast Atlantic during the Late Pleistocene and Holocene. *Earth Planet. Sci. Lett.* 233: 33–44.
- Duplessy, J. C., N. J. Shackleton, R. G. Fairbanks, L. Labeyrie, D. W. Oppo, and N. Kallel. 1988. Deep water source variations during the last climatic cycle and their impact on the global deep water circulation. *Paleoceanography* 3: 343–360.
- Edwards, R. L., J. H. Chen, and G. J. Wasserburg. 1986. ²³⁸U-²³⁴U-²³⁰Th-²³²Th systematics and the precise measurement of time over the past 500 000 years. *Earth Planet. Sci. Lett.* 81: 175–192.
- Frank, N., M. Paterne, L. Ayliffe, T. van Weering, J. P. Henriot, and D. Blamart. 2004. Eastern North Atlantic deep-sea corals: tracing upper intermediate water Delta C-14 during the Holocene. *Earth Planet. Sci. Lett.* 219: 297–309.
- Freiwald, A. 2002. Reef-forming cold-water corals. Pages 365–385 in G. Wefer, D. Billett, D. Hebbeln, G. Wefer, D. Billett, D. Hebbeln, B. B. Jørgensen, M. Schlüter, and T. C. E. van Weering, eds. *Ocean Margin System*, Springer.
- Gallup, C. D., R. L. Edwards, and R. G. Johnson. 1994. The timing of high sea levels over the past 200 000 years. *Science* 263: 796–800.
- Ganachaud, A. and C. Wunsch. 2000. Improved estimates of global ocean circulation, heat transport and mixing from hydrographic data. *Nature* 408: 453–457.
- Goldstein, S. J., D. W. Lea, S. Chakraborty, M. Kashgarian, and M. T. Murrell. 2001. Uranium-series and radiocarbon geochronology of deep-sea corals: Implications for Southern Ocean ventilation rates and the oceanic carbon cycle. *Earth Planet. Sci. Lett.* 193: 167–182.
- Groote, P. M., M. Stuiver, J. W. C. White, S. Johnsen, and J. Jouzel. 1993. Comparison of oxygen isotope records from the GISP2 and GRIP Greenland ice cores. *Nature* 366: 552–554.
- Heinrich, H. 1988. Origin and consequences of cyclic ice rafting in the northeast Atlantic Ocean during the past 130 000 years. *Quat. Res.* 29: 142–152.

- Hemming, S. R. 2004. Heinrich events: Massive late Pleistocene detritus layers of the North Atlantic and their global climate imprint. *Rev. Geophys.* 42 doi:10.1029/2003RG000128.
- Henderson, G. M. 2002. Seawater (234U/238U) during the last 800 thousand years. *Earth Planet. Sci. Lett.* 199: 97–110.
- Hughen, K. A., J. T. Overpeck, L. C. Peterson, and S. Trumbore. 1996. Rapid climate changes in the tropical Atlantic region during the last deglaciation. *Nature* 380: 51–54.
- Imbrie, J., J. D. Hays, D. G. Martinson, A. McIntyre, A. C. Mix, J. J. Morley, N. G. Pisias, W. L. Prell, and N. J. Shackleton. 1984. The orbital theory of Pleistocene climate: support from a revised chronology of the marine delta O-18 record. Pages 269–305 in A. Berger, J. Imbrie, J. Hays, G. Kukla, and B. Salzman, eds. *Milankovitch and Climate*. Proc. NATO workshop, Reidel; NATO ASI Series C 126.
- Mangini, A., M. Lomitschka, R. Eichstadter, N. Frank, S. Vogler, G. Bonani, I. Hajdas, and J. Patzold. 1998. Coral provides way to age deep water. *Nature* 392: 347–348.
- Marchitto, T. M., Jr., W. B. Curry, and D. W. Oppo. 1998. Millennial-scale changes in North Atlantic circulation since the last glaciation. *Nature* 393: 557–561.
- McManus, J. F., R. Francois, J. M. Gherardi, L. D. Keigwin, and S. Brown-Leger. 2004. Collapse and rapid resumption of Atlantic meridional circulation linked to deglacial climate changes. *Nature* 428: 834–837.
- Meibom, A., M. Stage, J. Wooden, B. R. Constantz, R. B. Dunbar, A. Owen, N. Grumet, C. R. Bacon, and C. P. Chamberlain. 2003. Monthly Strontium/Calcium oscillations in symbiotic coral aragonite: Biological effects limiting the precision of the paleotemperature proxy. *Geophys. Res. Lett.* 30 (7): Article # 1418. doi:10.1029/2002GL01686.
- Mix, A., E. Bard, and R. Schneider. 2001. Environmental processes of the ice age: land, oceans, glaciers (EPILOG). *Quat. Sci. Rev.* 20: 627–658.
- Oppo, D. W. and S. J. Lehman. 1993. Mid-Depth Circulation of the Subpolar North-Atlantic During the Last Glacial Maximum. *Science*: 1148–1152.
- Rahmstorf, S. 1995. Bifurcations of the Atlantic thermohaline circulation in response to changes in the hydrological cycle. *Nature* 378: 145–149.
- Robinson, L. F., N. S. Belshaw, and G. M. Henderson. 2004. U and Th concentrations and isotope ratios in modern carbonates and waters from the Bahamas. *Geochim. Cosmochim. Acta* 68: 1777–1789.
- _____, G. M. Henderson, and N. C. Slowey. 2002. U-Th dating of marine isotope stage 7 in Bahamas slope sediments. *Earth Planet. Sci. Lett.* 196: 175–187.
- _____, G. M. Henderson, L. Hall, and I. Matthews. 2004. Climatic control of riverine and Seawater uranium-isotope ratios. *Science*. 305: 851–854.
- _____, J. F. Adkins, D. P. Fernandez, D. S. Burnett, S.-L. Wang, A. Gagnon, and N. Krakauer. 2006. Primary U-distribution in scleractinian corals and its implications for U-series dating. *Geochem. Geophys. Geosyst.* 7: Q05022, doi:10.1029/2005GC001138.
- _____, J. F. Adkins, L. D. Keigwin, J. Southon, D. P. Fernandez, S.-L. Wang, and D. S. Scheirer. 2005. Radiocarbon variability in the Western North Atlantic during the last deglaciation. *Science* 310: 1469–1473.
- Schröder-Kitzrau, A., A. Freiwald, and A. Mangini. 2005. U/Th-dating of deep-water corals from the eastern North Atlantic and the western Mediterranean Sea. Pages 157–172 in A. Freiwald and J. Roberts, eds. *Cold-water corals and ecosystems*, Springer.
- _____, A. Mangini, and M. Lomitschka. 2003. Deep-sea corals evidence periodic reduced ventilation in the North Atlantic during the LGM/Holocene transition. *Earth Planet. Sci. Lett.* 216: 399–410.
- Shen, G. T. and E. A. Boyle. 1988. Determination of lead, cadmium and other trace-metals in annually-banded corals. *Chem. Geol.* 67: 47–62.
- Smith, J. E., M. J. Risk, H. P. Schwarcz, and T. A. McConnaughey. 1997. Rapid climate change in the North Atlantic during the Younger Dryas recorded by deep-sea corals. *Nature* 386: 818–820.

Stirling, C. H., T. M. Esat, M. T. McCulloch, and K. Lambeck. 1995. High-precision U-series dating of corals from Western Australia and implications for the timing and duration of the last interglacial. *Earth Planet. Sci. Lett.* 135: 115–130.

ADDRESSES: (L.F.R.) *Department of Marine Chemistry and Geochemistry, Wood Hole Oceanographic Institution, Woods Hole, Massachusetts 02543.* (D.S.S.) *US Geological Survey, 345 Middlefield Rd., MS989, Menlo Park, California 94025.* (J.F.A., D.P.F., A.G.) *CaltechMS 100-23, 1200 E. California Blvd., Pasadena, California 91125.* (R.G.W.) *Department of Biology, Wood Hole Oceanographic Institution, Woods Hole, Massachusetts 02543.* CORRESPONDING AUTHOR: (L.F.R.): *E-mail: <lrobinson@whoi.edu>.*

